Theory of the electron distribution function in a Lorentz gas at high E/n_0

K.-U. Riemann
Institut für Theoretische Physik, Ruhr-Universität Bochum, D-4630 Bochum 1, Germany
(Received 14 May 1992)

The stationary electron Boltzmann equation is solved for high reduced electric-field strengths E/n_0. We consider both the cases of a homogeneous system and of a Townsend ionization avalanche (exponentially growing electron density). The usual calculation scheme based on the two-term spherical-harmonic expansion fails due to the formation of runaway electrons at high energies. To account for this effect, the velocity space is separated into different energy regions. For energies below the "runaway threshold" ($v < v_R$) Boltzmann's equation is solved by a modification of the usual calculation scheme. The expansion breaks down near the runaway threshold. For $v > v_R$ we construct an alternative expansion that is suitable to describe the formation of a runaway beam. In the homogeneous case, the runaway flux excludes exactly stationary solutions. Under avalanche conditions, the runaway effect is "hidden" because the runaways follow a Maxwellian distribution. Nevertheless, it has a distinct influence on the ionization coefficient α. This is demonstrated with numerical results for a weakly ionized He plasma, where α decreases strongly with E for high E/n_0 values.

PACS number(s): 51.10.+y, 51.50.+v, 52.20.Fs, 52.80.Dy

I. INTRODUCTION

The knowledge of the electron-velocity distribution function (EVDF) is of principal importance for plasma and discharge modeling because it controls the current transport and the rates of nearly all elementary processes in the plasma. There are essentially two competing ways to calculate the EVDF. The most direct way, a Monte Carlo particle simulation, is in principle suitable to account for various conditions and effects, but has the disadvantage of a large expense in computation time. Moreover, due to the limited number of test particles, it gives only poor information on the most important high-energy tail of the EVDF. The alternative way, the solution of Boltzmann's equation, is in general quite complicated and depends in most case on reasonable approximations.

The most common approximation to calculate the EVDF is the two-term "spherical-harmonic expansion" (SHE) [1,2]. It accounts only for small deviations from an isotropic EVDF and is based on the assumptions of small gradients and of a small ratio $\nu_\varepsilon/\nu_1 = O(\epsilon)$ of the energy- and momentum-exchange collision frequencies (Lorentz-gas model). In the case of a homogeneous plasma dominated by elastic electron-atom collisions, these assumptions are well established ($\epsilon = m/M$) and result in the well-known Davydov distribution [3]. With increasing importance of inelastic collisions (and/or growing inhomogeneity), however, the anisotropy of the EVDF grows, and the two-term SHE becomes somewhat questionable. Nevertheless, it is the basis of nearly all usual EVDF computer codes (see, e.g., [4]). On the one hand, this is justified by the lack of sufficiently effective alternative procedures. On the other hand, calculations using a multiterm expansion indicate that the two-term SHE is (for not-too-high E/n_0) actually better than it should be [5,6].

There is one more principal limitation restricting the validity of the two-term SHE: For sufficiently high electron velocities v, all electron-collision cross sections decrease so fast that the field acceleration can no longer be balanced by collisional friction. This "runaway effect" was first described by Dreicer [7] for the fully ionized Coulomb system (with a collision cross section decreasing like $v^{-4}\ln v$). Ecker and Müller [8,9] could show that the runaway effect also exists in weakly ionized plasmas, where the electrons are governed by the interaction with neutral atoms. In contrast to the Coulomb system, however, it is restricted to very high electron velocities and is important only for high reduced field strengths E/n_0.

Strictly speaking, the runaway effect not only destroys the isotropy of the EVDF, but it also excludes stationary *and* homogeneous solutions of the electron Boltzmann equation (see Sec. III). Accounting for the spatial inhomogeneity of a Townsend ionization avalanche, Lagushenko and Maya [10] found reasonable stationary solutions of the electron Boltzmann equation, which could be described by the two-term SHE up to the highest E/n_0 values. This is in contrast to intuitive expectations and to widely used one-dimensional models of the EVDF in the cathode fall [11]. Lagushenko and Maya conceded the *a priori* limitation of the two-term ansatz and left the question open as to whether or not the runaway phenomenon exists under avalanche conditions.

We shall show in this paper that the runaway phenomenon does indeed exist, but is to some extent "hidden" under avalanche conditions. To investigate this, it is advantageous to start from the analysis of homogeneous systems and to generalize the results to avalanches. To describe the runaway formation correctly, the effect of forward scattering in inelastic collisions must be accounted for. The bulk of the EVDF can be described by the usual two-term SHE, but the runaway formation requires modified boundary conditions. For the

high-energy tail we construct an approximation which is suitable to describe the beam formation. The growing anisotropy of the EVDF results in a strong decrease of the Townsend ionization coefficient with increasing E/n_0. The general analysis is illustrated with numerical results for a simple model adapted to a weakly ionized He plasma.

II. BASIC EQUATIONS

We consider a stationary partially ionized Lorentz plasma with uniform neutral-particle density in a constant electric field **E**. The EVDF is homogeneous or depends only on the space coordinate z in the field direction. We use the notation

$$v=|\mathbf{v}|,\quad \mu=\frac{\mathbf{v}\cdot\mathbf{E}}{vE}=\frac{v_z}{v},\quad \text{and}\quad F=\frac{e}{m}|\mathbf{E}|\ , \tag{1}$$

where **v** is the velocity and e/m the charge-to-mass ratio of the electrons. To calculate the electron distribution function $f(z,v,\mu)$, we start from Boltzmann's equation,

$$\mu v\frac{\partial f}{\partial z}+\mu F\frac{\partial f}{\partial v}+(1-\mu^2)\frac{F}{v}\frac{\partial f}{\partial \mu}=C[f]\ . \tag{2}$$

For the formulation of the collision operator $C[f]$, it is convenient to refer to the SHE

$$f(z,v,\mu)=\sum_{n=0}^{\infty} f^n(z,v)P_n(\mu),\quad C[f]=\sum_{n=0}^{\infty} C^nP_n(\mu)\ , \tag{3}$$

where $P_n(\mu)$ designates the Legendre polynomial [12] of order n. For later use, we note the explicit formula

$$f^n(z,v)=\frac{2n+1}{2}\int_{-1}^{1} f(z,v,\mu)P_n(\mu)d\mu \tag{4}$$

for the expansion coefficients f^n. Introducing the expansion (3) into Boltzmann's' equation results in the hierarchy of kinetic equations [1,2]

$$\frac{v}{3}\frac{\partial f^1}{\partial z}+\frac{F}{3}\frac{1}{v^2}\frac{\partial}{\partial v}(v^2f^1)=C^0\ , \tag{5}$$

$$v\frac{\partial}{\partial z}\left\{\tfrac{2}{5}f^2+f^0\right\}+F\left[\frac{2}{5}\frac{1}{v^3}\frac{\partial}{\partial v}(v^3f^2)+\frac{\partial f^0}{\partial v}\right]=C^1\ ,$$

$$\vdots \tag{6}$$

$$v\frac{\partial}{\partial z}\left\{\frac{n+1}{2n+3}f^{n+1}+\frac{n}{2n-1}f^{n-1}\right\}+F\left[\frac{n+1}{2n+3}\frac{1}{v^{n+2}}\frac{\partial}{\partial v}(v^{n+2}f^{n+1})+\frac{n}{2n-1}v^{n-1}\frac{\partial}{\partial v}\frac{f^{n-1}}{v^{n-1}}\right]=C^n$$

$$\vdots\ . \tag{7}$$

Restricting ourselves to the Lorentz-gas approximation, we neglect energy exchange in the nonisotropic scattering terms and write [1]

$$C^n=C^n[f^n]=-\nu_n(v)f^n(z,v)=-n_0vq_n(v)f^n(z,v)\qquad (n\geq 1) \tag{8}$$

with

$$q_n(v)=2\pi\int_0^{\pi}\sigma(v,\theta)[1-P_n(\cos\theta)]\sin\theta\,d\theta\ ,$$

where σ is the differential cross section for collisions with deflection angle θ. According to the model of the Lorentz gas, electron scattering should be dominated by elastic encounters with atoms ($\sigma\approx\sigma_{\rm el}$). Actually, however, at high velocities, scattering by inelastic collisions cannot be neglected and is usually included in σ. In doing so, it is important to account for the effect of dominating forward scattering in elastic *and* inelastic collisions (see Appendix A).

The isotropic collision term C^0 describing energy exchange has to account for elastic (el) and inelastic (in) collisions with neutral atoms and for electron-electron encounters (*ee*). We write

$$C^0=C^0_{\rm el}+C^0_{ee}+\sum_{\rm in}C^0_{\rm in} \tag{9}$$

and use the following standard collision integrals:

(i) Elastic collisions [1,2]:

$$C^0_{\rm el}=\frac{1}{4\pi v^2}\frac{\partial S_{\rm el}}{\partial v} \tag{10}$$

with

$$S_{\rm el}=4\pi\frac{m}{M}n_0v^4q_{1\,\rm el}(v)\left[f^0+\frac{kT_0}{mv}\frac{\partial f^0}{\partial v}\right]\ ,$$

where n_0 is the neutral-particle density, M the mass, and $q_{1\,\rm el}$ the elastic momentum-exchange (transport) cross section defined by Eq. (8) (with $\sigma=\sigma_{\rm el}$). The neutral thermal energy kT_0 may be neglected in our case ($T_0\ll T_e$, where T_e denotes the electron temperature).

(ii) Electron-electron collisions [1,13]:

$$C^0_{ee}=\frac{1}{4\pi v^2}\frac{\partial S_{ee}}{\partial v}\ , \tag{11}$$

with

$$S_{ee}=4\pi v^4q_{ee}(v)\left[Af^0+Bv\frac{\partial f^0}{\partial v}\right]\ ,$$

and

$$A(v)=4\pi\int_0^v u^2f^0(z,u)du\to n_e\ ,$$

$$B(v)=\frac{4\pi}{3}\left[\frac{1}{v^2}\int_0^v u^4f^0(z,u)du+v\int_v^{\infty}uf^0(z,u)du\right]\to n_e\frac{kT_e}{mv^2}\ ,$$

$$q_{ee}(v)=\frac{e^4}{4\pi\epsilon_0m^2v^4}\ln\Lambda\ ,$$

where $\Lambda\sim 10$ is the Coulomb logarithm. The limiting values $A\to n_e$ (electron density) and $B\to n_ekT_e/mv^2$

($v \to \infty$) may be useful for convenient estimates and for simplifications. The Lorentz-gas model requires a low degree of ionization with $n_e q_{ee} \ll n_0 q_1$.

(iii) Inelastic collisions [14]:

$$C^0_{\text{in}} = n_0 \left\{ \frac{v^2_{+\text{in}}}{v} q_{\text{in}}(v_{+\text{in}}) f^0(v_{+\text{in}}) - v q_{\text{in}}(v) f^0(v) \right\} + \frac{g_0}{g_{\text{in}}} n_{\text{in}} \left\{ v q_{\text{in}}(v) f^0(v_{-\text{in}}) - \frac{v^2_{+\text{in}}}{v} q_{\text{in}}(v_{+\text{in}}) f^0(v) \right\} , \quad (12)$$

with

$$v^2_{\pm\text{in}} = v^2 \pm 2\varepsilon_{\text{in}}/m \ .$$

Here, the density of atoms in the ground state is identified with the neutral-particle density n_0. n_{in} designates the density of atoms in the considered excited state, g_0 and g_{in} are the corresponding statistical weights, and q_{in} is the total cross section for the excitation of the level in with excitation energy ε_{in}. (For the sake of simplicity, we have restricted ourselves to excitation from the ground state; a generalization is trivial.) We shall also use Eq. (12) to account for ionization. This approximation implies that the secondary electron appears at low energy and can be neglected. (For a detailed discussion, see Ref. [15].)

The elastic and electron-electron collision terms exhibit *a priori* the typical Fokker-Planck form $v^{-2}\partial S/\partial v$, indicating that the small energy exchange in encounters can be represented by the divergence of a flux in velocity space. To solve Boltzmann's equation, it is convenient to represent the inelastic contribution to the same form. We therefore write

$$C^0[f^0] = \frac{1}{4\pi v^2} \frac{\partial S}{\partial v} , \quad (13)$$

with

$$S(z,v) = S_{\text{el}} + S_{ee} + \sum_{\text{in}} S_{\text{in}} ,$$

and calculate from Eq. (12) the inelastic contributions

$$S_{\text{in}} = 4\pi n_0 \int_v^{v_{+\text{in}}} u^3 q_{\text{in}}(u) \times \left\{ f^0(z,u) - \frac{g_0 n_{\text{in}}}{g_{\text{in}} n_0} f^0(z, u_{-\text{in}}) \right\} , \quad (14)$$

where $u_{-\text{in}}$ is defined in analogy to $v_{-\text{in}}$. Cutting the kinetic hierarchy (5)–(7) at a suitable index m (i.e., $f^{m+1}=0$; in the usual two-term SHE, one has $m=1$) and inserting the collision terms (8)–(14) results in a system of integro-differential equations for f. In general, this system can be solved by matrix methods or by an iteration process involving standard differential equation techniques.

The numerical evaluation is decisively facilitated if electron-electron collisions ($n_e \to 0$) and collisions of the second kind ($n_{\text{in}} \to 0$) can be neglected: In this case, $S(z,v)$ depends on $f^0(z,u)$ only for velocities $u \geq v$ [see Eqs. (11) and (14)] and can be determined successively by backward integration without iteration. In our numerical illustrations referring to a weakly ionized He plasma, we will make use of this simplification. For the sake of clearness, we shall further consider one effective inelastic process only. The electron-collision cross sections used are shown in Fig. 1; for details see Appendix A. We would like to point out, however, that the principal analysis and the conclusions do *not* depend on these simplifications.

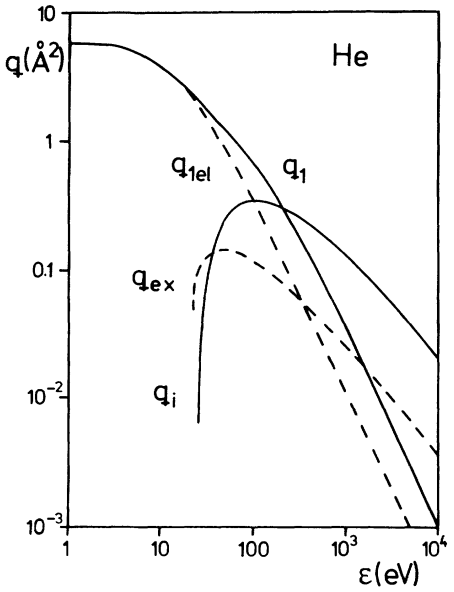

FIG. 1. Electron collision cross sections in He (see Appendix A): $\varepsilon = mv^2/2$, $q_{\text{ex,i}}$ = total cross sections for excitation and ionization; and $q_{1(\text{el})}$ = (elastic) momentum-transfer cross section.

III. THE RUNAWAY EFFECT

We consider the hierarchy (5)–(7) for homogeneous ($\partial/\partial z = 0$) systems. In the simplest case of only elastic electron-atom collisions ($C^0 = C^0_{\text{el}}$, $T_0 = 0$), the two-term SHE ($f^2 = 0$) results in the well-known Davydov distribution [3] [cf. Eqs. (5), (6), and (10)]

$$f^0(v) = f^0(0) \exp\left\{ -\frac{3m}{F^2 M} \int_0^v \nu_1^2(u) u \, du \right\} . \quad (15)$$

As pointed out by Levinson [16] and Stenflo [17], it is obvious that f^0 does not tend to zero and cannot be normalized if $\nu_1(v)$ decreases faster with v than $1/v$. Corresponding results are also obtained if other collision processes are taken into account. Conclusions relating this difficulty to the runaway effect are questionable due to the breakdown of the two-term SHE. Avoiding this expansion, Cavalleri and Paveri-Fontana [18] have shown that the stationary and homogeneous Boltzmann equation has no physical solution, (i.e., a solution which can be normalized) if the integral

$$I(v) = \int_v^\infty \nu_t(u) du \quad (16)$$

exists, i.e., if the *total* collision frequency $\nu_t(v)$ decreases faster than $1/v$ for $v \to \infty$. This breakdown of a stationary and homogeneous electron distribution function was explained with the runaway effect.

Indeed, if $I(v)$ exists, we find a finite probability

$$p_R(v) = \exp[-I(v)/F] \tag{17}$$

for an electron moving with velocity v in the field direction to be continuously accelerated without ever colliding, i.e., to "run away." On the other hand, we expect that the runaway phenomenon depends not only on the number, but also on the efficiency, of collisions. To make this clear, we can use a simple picture given by Ecker and Müller [8] to compare the field acceleration F of an electron moving with velocity v in the field direction and its mean deceleration $v\nu_1(v)$ by collisions. The ratio

$$\rho(v) = \frac{v\nu_1(v)}{F} \tag{18}$$

depends not on the *total* but on the *momentum-transfer* collision frequency ν_1 [cf. Eq. (8)]. Electrons with $\rho(v) < 1$ experience an average net acceleration, and they will "run away" if $\rho(u) < 1$ holds for *all* $u \geq v$.

Actually, due to the intrinsic Coulomb nature of *all* electron interactions, we must expect that all collision cross sections decrease faster than $1/v^2$ so that we have $\rho(v) < 1$ for sufficiently large v. Using the cross section q_1 of Fig. 1, this is illustrated in Fig. 2 for the case of a large reduced field strength $E/n_0 = 500$ Td (1 Td $= 10^{-17}$ V cm^2) in He. The momentum balance $\rho(v) = 1$ is fulfilled at two different velocities, $v = v_D$ and $v = v_R$. v_D represents the drift velocity, and v_R designates the runaway velocity threshold beyond which electrons can no longer be slowed down by collisions. Of course, this simple picture has to be refined to account for the correct distribution of velocities v and velocity directions $\mu = v_z/v$. Actually, the greater part of the electrons is captured with $\rho > 1$ at the left-hand side (LHS) of the "hump" shown in Fig. 2. Some electrons, however, attain velocities $v > v_R$ and become runaways. (It is illustrative to compare the runaway formation in velocity space with the quantum-mechanical tunnel effect in configuration space.) In principle, runaways can be generated at arbitrary field strengths. The energy threshold presented in Table I shows, however, that the effect is practically restricted to high reduced field strength E/n_0.

TABLE I. Runaway energy limit $\varepsilon_R = mv_R^2/2$; $(E/n_0)_{cr} = 1309$ Td.

E/n_0 (Td)	ε_R (keV)
120	22.9
150	16.0
200	9.98
300	5.04
500	2.00
750	0.875
1000	0.427
1200	0.226
(1309)	(0.105)

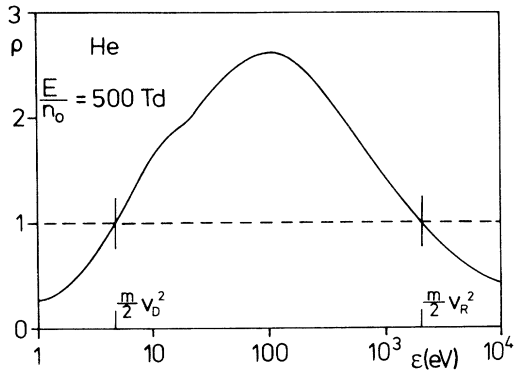

FIG. 2. Momentum balance of the electrons: $\rho = mv\nu_1(v)/eE$, $\varepsilon = mv^2/2$.

For extremely high fields exceeding a critical value $(E/n_0)_{cr} = 1309$ Td, finally, *all* electrons are runaways. This intrinsically nonstationary case is beyond the scope of our interest.

From the above discussion we expect that the runaway condition $v\nu_t(v) \to 0$ of Cavalleri and Paveri-Fontana [18] should be replaced by the weaker condition that there is a velocity threshold v_R with

$$\rho(v) = \frac{v\nu_1(v)}{F} = \frac{n_0}{F} v^2 q_1(v) < 1 \quad \text{for all } v > v_R \ . \tag{19}$$

To prove this, we consider the second equation of the kinetic hierarchy (5)–(7) without neglecting f^2. Searching for a stationary and homogeneous solution, we obtain from Eqs. (6) and (8)

$$\frac{2}{5}\frac{d}{dv}(v^3 f^2) + v^3 \frac{df^0}{dv} = -\rho(v) v^2 f^1 \ . \tag{20}$$

Integrating Eq. (20) and observing $\rho < 1$, we have for $v > v_R$

$$-\tfrac{2}{5}v^3 f^2 - v^3 f^0 - 3\int_v^\infty u^2 f^0(u)\,du > -\int_v^\infty u^2 |f^1(u)|\,du \ . \tag{21}$$

The existence of the integrals follows if we assume that the distribution function can be normalized. With $P_0 = 1$ and $P_1 = \mu$, we find from Eq. (4)

$$|f^1(v)| \leq \tfrac{3}{2}\int_{-1}^{1} |\mu| f(v,\mu)\,d\mu \leq \tfrac{3}{2}\int_{-1}^{1} f(v,\mu)\,d\mu = 3f^0(v) \tag{22}$$

and arrive at

$$f^2(v) < -\tfrac{5}{2} f^0(v) \ . \tag{23}$$

This inequality not only indicates the breakdown of the two-term SHE, but it also is not consistent with Eq. (4): With

$$P_2(\mu) = (3\mu^2 - 1)/2 \geq -\tfrac{1}{2} \ ,$$

we have, in contradiction to Eq. (23),

$$f^2(v) \geq -\tfrac{5}{2}\int_{-1}^{1} f(v,\mu)\tfrac{1}{2}d\mu = -\tfrac{5}{2}f^0(v) \ . \tag{24}$$

Remembering the assumptions of the proof, the contradiction shows that the stationary and homogeneous Boltzmann equation has no solution which can be normalized if the runaway condition (19) is fulfilled.

IV. HOMOGENEOUS ELECTRON DISTRIBUTION

In this section we follow in some aspects a corresponding analysis for fully ionized systems given by Gurevich [19] and by Lebedev [20]. Looking for a stationary and homogeneous solution of Boltzmann's equation, we have to give up the normalization. The comparison of the runaway effect with the tunnel effect in quantum mechanics helps to understand this: In place of a distribution function describing a given particle density, we consider a distribution function describing a given particle flux S_R to infinity in velocity space or, equivalently, a given divergence of the current density in configuration space. Formally, this is achieved by integrating Eqs. (5) and (13) in the form

$$\frac{4\pi}{3}Fv^2 f^1(v) = S(v) + S_R \tag{25}$$

with an integration constant $S_R \neq 0$. The LHS of this equation describes the number of electrons flowing per unit volume and unit time through the surface of a sphere with radius v in velocity space. For $v \to \infty$ we have $S(v) \to 0$, and

$$S_R = \frac{4\pi}{3}F \lim_{v\to\infty} v^2 f^1(v) \tag{26}$$

is the rate at which electrons are "lost" to infinitely high velocities, i.e., the runaway rate. Of course, the "sink" at $v = \infty$ must, strictly speaking, produce a weak time dependence if it is not balanced by suitable sources. We shall assume such (artificial) sources at velocities too low to be of interest for us. This will result in a weak singularity for $v \to 0$ representing the particle influx.

A. Two-term spherical-harmonic expansion

Starting from this reinterpretation of the distribution function and the corresponding boundary condition (26) we ask for the validity of the two-term SHE. With

$$C^n = -\nu_n f^n = O(\rho F f^n / v)$$

(cf. Eqs. (8) and (18)], we estimate from the hierarchy (6) and (7) the order of magnitude

$$f^{n-1} = O(\rho f^n) \tag{27}$$

and note the condition $\rho \gg 1$. Making use of the Lorentz-gas assumption in the form

$$C^0 = O(\nu_e f^0) = O(\epsilon \nu_1 f^0) \ , \tag{28}$$

where ϵ is a smallness parameter characterizing the ratio of the energy- and momentum-exchange collision frequencies, we read from Eq. (25),

$$f^1(v) = \frac{3S_R}{4\pi F v^2} + O(\epsilon\rho f^0) \ . \tag{29}$$

In the "thermal" bulk of the distribution function ($v \approx v_{\rm th}$), which is governed by the balance of Ohmic heating and energy loss in collisions ("energy-loss region"), the runaway flux S_R may be neglected, and we have from Eqs. (27) and (29),

$$\rho(v_{\rm th}) = O(\epsilon^{-1/2}) \gg 1 \ . \tag{30}$$

This self-consistently established parameter value (and *not* a "small" electric field) provides the basis for the two-term SHE for the Lorentz gas. The expansion breaks down the "runaway region" $v \geq v_R$, with $\rho(v) \leq 1$. Between the energy-loss and the runaway regions, there is an intermediate parameter range $\rho \gg 1$, $\epsilon\rho^2 \ll 1$. In this region, which is dominated by angular scattering, the two-term SHE is still valid [see Eq. (27)]. On the other hand, energy loss in collisions can already be neglected, and f^1 is determined by the runaway flux S_R [see Eq. (29)]. The different regions in velocity space and their characteristic features are summarized in Table II.

Putting aside at the moment the analysis of the runaway region, we can therefore apply the two-term SHE and calculate f^0 and f^1 from

$$f^0(v) = \int_v^\infty \frac{\rho(u)}{u} f^1(u)du \tag{31}$$

[cf. Eq. (20), $f^2 = 0$] and from Eq. (25). Figure 3 shows results for the EVDF in a weakly ionized He plasma at high E/n_0. (Details of the numerical procedure are given in Appendix B.) We recognize distinctly the forma-

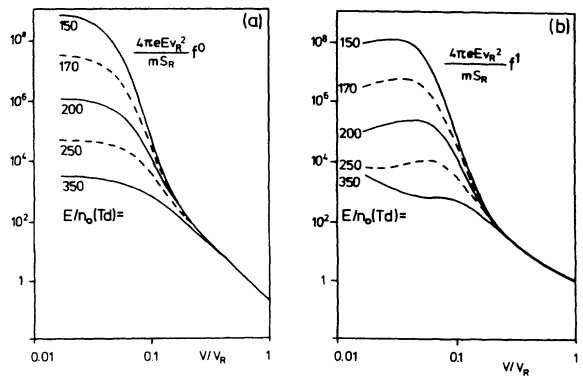

FIG. 3. Homogeneous electron distribution functions $f^0(v)$ and $f^1(v)$ in He.

TABLE II. Regions in velocity space: $\rho = mv\nu_1(v)/eE$, $\epsilon = O(\nu_\epsilon/\nu_1)$.

Region	Energy Loss	Angular scattering	Runaway
Parameter range	$\rho \gg 1$, $\epsilon\rho^2 \sim 1$	$\rho \gg 1$, $\epsilon\rho^2 \ll 1$	$\rho \leq 1$
Electron distribution	Nearly isotropic $f^2 \ll f^0$; Usual calculations		Anisotropic $f^1 = \frac{3mS_R}{4\pi eEv^2}$

tion of the energy-loss region controlled by collisional cooling and of the angular scattering region dominated by the runaway loss. The normalization used in Fig. 3 expresses a similarity law for the EVDF in this latter zone: Assuming a power law

$$\rho(v) = (v_R/v)^\alpha \tag{32}$$

in the scattering region, we obtain from Eqs. (29) and (31),

$$f^0(v) = \frac{1}{\alpha+2}\left[\frac{v_R}{v}\right]^\alpha f^1(v) \tag{33}$$

with

$$f^1(v) = \frac{3S_R}{4\pi F v_R^2}\left[\frac{v_R}{v}\right]^2 .$$

With the cross sections for He given in Appendix A, we have $\alpha \approx 1$. Consequently, we find $f^1 \approx 3f^0$ at the runaway threshold v_R. Naturally, at this point the validity of the two-term SHE is already exceeded. For low velocities $v \ll v_R$, we expect from Eq. (33), $f^1 \ll f^0$. Actually, the numerical results presented in Fig. 3 show that this is only poorly fulfilled. The reason for this is *not* the runaway effect but the limited validity of the Lorentz-gas assumptions for energies above the excitation energy [cf. the discussions in Sec. I and after Eq. (8)].

B. Beam formation

The relation of the runaway flux and of f^1 given by Eq. (26) is exact and does *not* depend on the two-term SHE. The corresponding asymptotic form of f^1, however, is already established in the angular scattering region, where the two-term SHE is still valid. Consequently, to determine the runaway flux and the distribution function of nonrunaways, there is not need to drop the two-term SHE and to study the runaway region. On the other hand, the beam formation of runaway electrons is *per se* interesting, and therefore we do not care about the practical importance.

To calculate the EVDF in the runaway region, we cannot cut the hierarchy and need, in principle, a detailed knowledge of the differential collision cross section $\sigma(v,\theta)$ or, equivalently, of *all coefficients* $\nu_n(v)$ [see Eq. (8)]. To come to a tractable mathematical formulation, we make use of the fact that forward scattering with small deflection angle θ is predominant at high energies. This enables us to approximate the Boltzmann collision term $C[f]$ in the differential Fokker-Planck form [21]. Neglecting energy loss in the runaway region (cf. Table II), we find in Appendix C,

$$C[f] = \tfrac{1}{2}\nu_1(v)\frac{\partial}{\partial\mu}\left[(1-\mu^2)\frac{\partial f}{\partial\mu}\right] . \tag{34}$$

Introducing this collision term into Eq. (2) and using Eq. (18), we obtain the kinetic equation

$$\mu v\frac{\partial f}{\partial v} + (1-\mu^2)\frac{\partial f}{\partial\mu} = \tfrac{1}{2}\rho(v)\frac{\partial}{\partial\mu}\left[(1-\mu^2)\frac{\partial f}{\partial\mu}\right] . \tag{35}$$

A further simplification is achieved if we restrict ourselves to the vicinity of the field axis $\mu = 1$, where we expect to observe the beam formation (cf. also [19,20]). Linearizing in $1-\mu$ and introducing the dimensionless variables

$$x = \frac{1}{v_R^2}\int^v v\rho(v)dv \quad \text{and} \quad y = \frac{v^2}{v_R^2}\frac{1-\mu}{x} , \tag{36}$$

we arrive at the parameter-free universal kinetic equation

$$x\frac{\partial f}{\partial x} = (1+y)\frac{\partial f}{\partial y} + y\frac{\partial^2 f}{\partial y^2} . \tag{37}$$

For all usual collision cross sections decreasing faster than v^{-2} and slower than v^{-4} with v, we have $x \to \infty$ and $y \to \infty$ ($\mu < 1$) for $v \to \infty$. Equation (37) can obviously be solved by separation and we find the special solutions

$$f^{(\nu)}(x,y) = x^{-\nu-1}e^{-y}L_\nu(y) , \tag{38}$$

where L_ν designates the νth-order Laguerre polynomial [22]. [According to the completeness of the system (38), we have restricted ourselves here to non-negative integer ν; separation solutions for arbitrary ν can be expressed in terms of hypergeometric functions.] From Eqs. (26) and (4), we calculate the contribution

$$S_R^{(\nu)} = 2\pi F v_R^2 \lim_{\substack{x=x(v)\\ v\to\infty}}\left[x\int_0^\infty\left[1-\frac{v_R^2}{v^2}xy\right]f^{(\nu)}(x,y)dy\right]$$
$$= 2\pi F v_R^2\,\delta_{\nu,0} \tag{39}$$

of $f^{(\nu)}$ to the runaway flux S_R. ($\delta_{\nu,0}$ designates the Kronecker symbol; using the differential equation for $f^{(\nu)}$, it can be verified that $S_R^{(\nu)}=0$ holds for *arbitrary* $\nu\neq 0$.) Consequently, the EVDF near the axis in the runaway region can be represented in the form

$$f(x,y)=\frac{S_R}{4\pi F v_R^2}e^{-y}\left[\frac{2}{x}+\frac{a_1}{x^2}L_1(y)+\frac{a_2}{x^3}L_2(y)+\cdots\right], \tag{40}$$

with

$$L_1(y)=1-y,\quad L_2(y)=1-2y+y^2/2,\ldots .$$

To get a consistent uniform representation, Eq. (40) has to be matched on the axis ($y=0$, $\mu=1$) with the SHE result [cf. Eqs. (29) and (31)]

$$f(v,\mu)=\frac{S_R}{4\pi F v_R^2}\left[3v_R^2\int_v^\infty\frac{\rho(u)}{u^3}du+3\mu\frac{v_R^2}{v^2}+O\left[\frac{v_R^2}{\rho v^2}\right]\right], \tag{41}$$

where we have used Eq. (27) to estimate the contribution of $f^2(v)$, which is neglected in the two-term expansion. In general, this matching will be difficult: The representations (40) and (41) refer to opposite parameter ranges $v>v_R$ and $v<v_R$, both breaking down for $v\sim v_R$. In the case of He with $\rho(v)=v_R/v$ [see Eqs. (32) and (33)], however, we have

$$x=\frac{v}{v_R},\quad y=\frac{v}{v_R}(1-\mu),\quad v_R^2\int_v^\infty\frac{\rho(u)}{u^3}du=\frac{1}{3}\frac{v_R^3}{v^3} \tag{42}$$

and can compare Eqs. (40) and (41) term by term with the result $a_1=3$ and $a_2=1$. [It should be noted that the leading term of Eq. (40) corresponds to the f^2 correction in Eq. (41). For other special cases, solutions with noninteger ν may be advantageous.]

The corresponding EVDF is presented in Fig. 4. According to the normalization used, the presentation does not depend on E/n_0. It should be observed, however, that the model assumptions used in the derivation assume

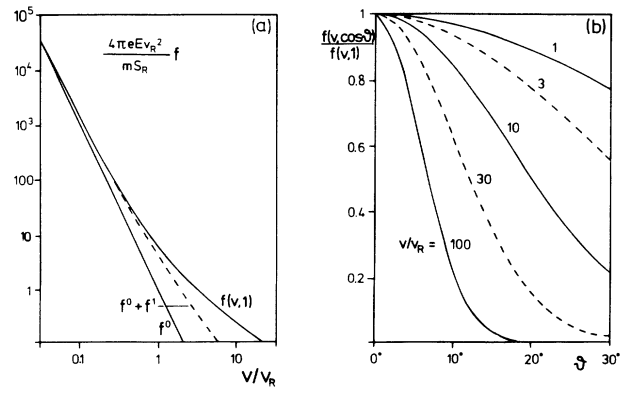

FIG. 4. Electron distribution function in the runaway region for $E/n_0<(E/n_0)_{cr}$: (a) Velocity distribution on the axis, matching with f^0+f^1 and (b) angular distribution, $\vartheta=\arccos\mu$.

$E/n_0<(E/n_0)_{cr}$. Figure 4(a) demonstrates the matching of Eq. (40) with $f^0(v)+f^1(v)$ on the axis ($y=0$) and Fig. 4(b) shows the angular distribution near the axis. In principle, we recognize distinctly the expected beam formation with increasing v. On the other hand, comparison with Table I shows that a sharp peak will actually not be formed: Velocities $v>10v_R$ (as displayed in the figure) can hardly be generated by the total voltage applied to a gas discharge (and if so, they require a relativistic analysis).

V. ELECTRONS IN A TOWNSEND AVALANCHE

Under runaway conditions, our proof in Sec. III excludes solutions of Boltzmann's equation which are stationary *and* homogeneous. Now we give up the homogeneity and consider the space dependence $f\propto\exp(\alpha z)$ of an ionization avalanche, i.e., we look for regular solutions of the equation [see Eq. (2)]

$$\mu\left[\alpha v f+F\frac{\partial f}{\partial v}\right]+(1-\mu^2)\frac{F}{v}\frac{\partial f}{\partial\mu}=C[f]\ . \tag{43}$$

Townsend's ionization coefficient α is not a free parameter but has to be determined self-consistently: Integrating Eq. (43) over all velocities (with $d^3v=2\pi v^2 dv\,d\mu$) results in $\alpha\langle v_z\rangle=\sigma$, where [cf. Eqs. (1) and (4)]

$$\langle v_z\rangle=\frac{1}{n_e}\int\mu v f\,d^3v=\frac{4\pi}{3n_e}\int v^3 f^1 dv \tag{44}$$

is the mean electron-flow velocity and

$$\sigma=\frac{1}{n_e}\int C[f]d^3v=4\pi\frac{n_0}{n_e}\int v^3 q_i f^0 dv \tag{45}$$

is the ionization rate. Consequently, when solving Eq. (43), we have to observe the condition

$$\alpha=\frac{\sigma}{\langle v_z\rangle}=3n_0\frac{\int_0^\infty v^3 q_i(v)f^0(z,v)dv}{\int_0^\infty v^3 f^1(z,v)dv}\ . \tag{46}$$

[To avoid confusion with similar expressions derived from special assumptions, we point out that Eq. (46) holds exactly and is neither restricted to small α nor based on the two-term SHE.]

A. Reduction to a homogeneous system

Equation (43) suggests utilizing energy conservation $Fz-v^2/2=\text{const}$ in characteristic orbits to eliminate the additional term $\alpha v f$ originating from the inhomogeneity. Starting from the ansatz

$$f(z,v,\mu)=\exp\left[\alpha z-\frac{\alpha}{2F}v^2\right]g(v,\mu) \tag{47}$$

results in

$$\mu F\frac{\partial g}{\partial v}+(1-\mu^2)\frac{F}{v}\frac{\partial g}{\partial\mu}=e^{(\alpha/2F)v^2}C[e^{-(\alpha/2F)v^2}g]$$
$$=\hat{C}[g]\ . \tag{48}$$

Obviously this equation is identical with the kinetic equa-

tion for stationary and homogeneous systems, except for the fact that the collision operator C is replaced by $\hat{C}$. Engaging again the SHE and the Lorentz-gas approximation [see Eq. (8)], we obtain

$$\hat{C}^0=\hat{C}^0[g^0]=e^{(\alpha/2F)v^2}C^0[e^{-(\alpha/2F)v^2}g^0]\ ,$$
$$\hat{C}^n=C^n[g^n]=-\nu_n(v)g^n(v)\quad (n\geq 1)\ . \tag{49}$$

This conservation of the *structure* of the collision term—which was the reason we used the *isotropic* invariant $Fz-v^2/2$ and *not* the invariant $Fz-v_z^2/2$—implies that we can utilize nearly the entire analysis of Sec. IV. In particular, the angular scattering region and the runaway region remain completely unchanged. We have merely to replace C^0 by $\hat{C}^0$ in the numerical evaluation of the energy-loss region. Physically, this means that particle exchange by diffusion is formally described in terms of a source in velocity space (without *local* particle conservation). Trivially, the ansatz (47) guarantees that f can be normalized (in contrast to g). Correspondingly,

$$\lim_{v\to\infty} v^2 g^1(v)=\frac{3S_R}{4\pi F} \tag{50}$$

[cf. Eq. (26)] can now be considered as an arbitrary normalization constant and does not directly describe the local runaway production rate.

We refer again to our simplified model of a weakly ionized He plasma and show some results in Table III and in Fig. 5. (For numerical details, see again Appendix B.) The influence of the inhomogeneity (α) on the distribution function may be characterized by $\alpha kT_e/eE$. As Table III shows, this influence is negligible for $E/n_0<30$ Td ($E/p_0<10$ V/cm Torr). For larger values of E/n_0, f and α must be determined consistently by iteration.

B. Approximations for high E/n_0

For sufficiently high E/n_0, the energy loss in collisions may be completely neglected, and we have in analogy to Eqs. (31) and (29), $g^0=-\int g^1\rho/v\,dv$ and $g^1\propto 1/v^2$. With Eqs. (19) and (47), we can write

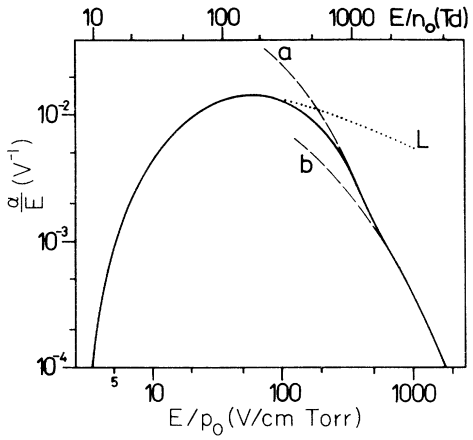

FIG. 5. Townsend ionization coefficient in He (solid line). L indicates the results of Lagushenko and Maya [10], a the approximation neglecting energy loss in collisions, and b the approximation neglecting all scattering. α/E is in V^{-1} and E/p_0 is in V/(cm Torr).

$$f^0=\frac{n_0}{F}v^2 f^1(v)G(v)\quad\text{and}\quad f^1\propto\frac{1}{v^2}e^{-\alpha/2Fv^2} \tag{51}$$

with

$$G(v)=\int_v^\infty q_1(u)\frac{du}{u}\ .$$

Introducing this into Eq. (46) results in the relation

$$\left[\frac{F}{n_0}\right]^2=3\int_0^\infty v^3 q_i(v)G(v)e^{-(\alpha/2F)v^2}dv\ , \tag{52}$$

expressing E/n_0 as a function of α/E. The result for He is shown in curve a of Fig. 5. At $E/n_0\approx 1000$ Td, it merges smoothly with the numerical curve discussed above.

For the case of an isotropic collision cross section varying inversely proportional to v (constant collision frequency), the above approximation becomes identical with

TABLE III. Electron temperature T_e, mean velocity $\langle v_z\rangle$, and ionization coefficient α in He: E/n_0 (in Td)$=2.829E/p_0$ (in V/cm Torr).

E/p_0 (V/cm Torr)	kT_e (eV)	$10^{-4}\langle v_z\rangle$ (ms^{-1})	$10^4\alpha/E$ (V^{-1})
1	1.22	0.91	3.8×10^{-14}
2	2.89	1.46	5.8×10^{-3}
5	4.78	3.59	8.10
10	5.60	7.13	43.8
20	6.73	14.1	95.0
40	8.66	28.0	134
70	11.9	48.4	144
100	15.5	71.9	129
150	23.2	112	104
200	32.9	162	79.5
250	45.2	224	59.9
300	56.9	297	45.0

a classical model of the ionization growth investigated by Gerjuoy and Stuart [23]. From this model it was predicted for the first time that α decreases with increasing E/n_0 for high E/n_0. In the analysis of Gerjuoy and Stuart, there is no upper limit in E/n_0 because there is no runaway effect for constant collision frequency. In our case, however, increasing E/n_0 further and exceeding the critical field $(E/n_0)_{cr} \approx 1300$ Td (see Table I), both the numerical result and Eq. (52) must fail, because they are based on the two-term SHE. This can be seen from the ratio $f^1/f^0 \to \infty$ for $F/n_0 \to \infty$, contradicting the necessary restriction $f^1 \leq 3f^0$ [see Eq. (22)].

As discussed with Eq. (33), the limiting ratio $f^1/f^0=3$ is met near the runaway threshold v_R, and the suggestion might be made to utilize the analysis of Sec. IV B to calculate g and f for $v > v_R$. This analysis, however, is again restricted to reduced field strengths $E/n_0 < (E/n_0)_{cr}$ because the expansion coefficients were determined by matching with the two-term SHE. Moreover, the representation of the EVDF in Sec. IV B is valid only in the vicinity of the field axis $\mu=1$ and is not suitable to determine the ratio f^1/f^0. We can, however, account for the runaway formation if we redefine $G(v)$ in Eqs. (51) and (52) by

$$G(v)=\max\left\{\int_v^\infty q_1(u)\frac{du}{u}, \frac{F}{3n_0v^2}\right\} \tag{53}$$

to enforce $f^0 \geq f^1/3$. This approximation was used to continue the solid curve of Fig. 5 beyond the critical field $(E/n_0)_{cr}$. The remaining uncertainty of f^0 near the runaway threshold v_R may be recognized from a small dent in the $\alpha(E)$ curve near the critical field.

The extreme runaway limit $f^0 \equiv f^1/3$ (i.e., $G = F/3n_0v^2$) resulting in

$$\frac{F}{n_0}=\int_0^\infty vq_i(v)e^{-(\alpha/2F)v^2}dv \tag{54}$$

is shown in curve b of Fig. 5. Interestingly, the same result is obtained from a one-dimensional description of the electrons starting from the kinetic equation

$$\alpha v_z f(z,v_z)+F\frac{\partial f}{\partial v_z}=\sigma\delta(v_z) \tag{55}$$

and neglecting scattering completely.

VI. SUMMARY AND DISCUSSION

Due to the strong decrease of the momentum-transfer collision cross section at high energies (see Fig. 1 for e-He collisions), the field acceleration $F=eE/m$ of sufficiently fast ($v > v_R$) electrons cannot be balanced by the mean collisional deceleration $v\nu_1(v)$ (see Fig. 2 and Table I). These electrons become "runaways." As we have seen in Sec. III, the runaway formation not only results in a breakdown of the two-term SHE at $v \approx v_R$, but also implies that the stationary and homogeneous electron Boltzmann equation has no solution which can be normalized. With modified boundary conditions in velocity space, however, it is possible to construct a stationary and homogeneous EVDF which is normalized with the runaway flux (production rate) S_R rather than with the electron density n_e (Sec. IV). Calculating this EVDF, three different regions in velocity space may be distinguished (cf. Table II), as follows.

(i) The energy-loss region I ($v \ll v_R$), which is governed by the balance of Ohmic heating and collisional cooling. In this region the runaway flux may be neglected.

(ii) The angular-scattering region II ($v < v_R$), which is governed by the balance of field acceleration and momentum loss in collisions. In this region the Ohmic heat is consumed in runaway formation.

(iii) The runaway region III ($v > v_R$), where the electrons are continuously accelerated and which is characterized by strong anisotropy and beam formation.

Accounting for the modified boundary condition (26) related to the runaway flux, in regions I and II the usual two-term SHE can be applied (Sec. IV A). The results for a weakly ionized He plasma presented in Fig. 3 reveal a similarity law for the EVDF in region II (and III). To calculate the EVDF in region III, we utilize the dominant forward scattering at high energies and start from an expansion of the electron Boltzmann equation in the vicinity of the field direction (Sec. IV B). The expansion coefficients are determined by adapting the runaway flux and matching the EVDF on the field axis [Fig. 4(a)]. The angular distribution of the electron velocities [Fig. 4(b)] shows the increasing anisotropy and gradual beam formation.

The homogeneous theory can be generalized for the case of inhomogeneous systems under Townsend avalanche conditions (Sec. V). In contrast to homogeneous systems, there exists a stationary EVDF which can be normalized in the usual sense. This is caused by a Maxwellian factor $\exp(-\alpha v^2/2F)$ supplementing the Boltzmann-like space dependence $\exp(\alpha z)$ (Sec. V A). The existence of a regular steady-state solution under runaway conditions might be explained by the idea that the electron density gradient drives the electrons in the direction opposite to the electric force [10]. Actually, however, the density gradient generates no real physical force acting on a single electron and impeding the runaway formation. From a mathematical point of view, the conception of field drift and diffusion is restricted to sufficiently isotropic EVDF's, and this means that the electric force must be essentially balanced by momentum loss in collisions.

Our analysis shows that the anisotropy of the EVDF in regions II and III—and, with that, the runaway formation—is not influenced by the space gradient. We can therefore state that the runaway phenomenon exists under Townsend avalanche conditions, but that the runaways are (nearly) Maxwell distributed. This Maxwellian distribution has nothing to do with thermal equilibrium or with a balance of diffusion and field drift. It reflects simply the energy conservation of the electrons in regions II and III [cf. Table II and Eq. (47)]: The number of high-energy electrons is exponentially small because they come from a region where the density is exponentially small.

To account for the runaway phenomeneon, the effect of forward scattering of high-energy electrons in elastic as

well as in *inelastic* collisions must be observed. (Assuming isotropic scattering results in a momentum-transfer cross section q_1 violating the runaway condition (19); see Fig. 1 and Appendix A.) The influence of the runaway formation on the Townsend ionization coefficient α can distinctly be seen from Fig. 5: For small and moderate reduced fields $E/n_0 < 300$ Td ($E/p_0 < 100$ V/cm Torr), our results for α/E agree with those of Lagushenko and Maya [10] (curve L), which were obtained from the same set of cross sections, but do not account for the runaway effect. For high E/n_0, however, our results deviate from curve L and show a strong decrease of the ionization coefficient. The decrease may be interpreted by the growing anisotropy. If the EVDF is nearly isotropic, electrons drifting in the field have a long mean free path and cause many ionization processes. This random walk is missing in an anisotropic distribution where the particles can follow the field direction [cf. the denominator in Eq. (46)]. The relation to the runaway effect may be confirmed from the approximations of Sec. V B (curves a and b in Fig. 5), which are explicitly based on the runaway conception.

The ionization probability in a Townsend discharge with finite electrode distance d may be nonuniform [9,24,25] and may be different from that in an infinitely extended avalanche. Nevertheless, the temptation to point out the effect of the decreasing ionization coefficient on Paschen's law is too strong. Disregarding ionization by ions and fast atoms [26] and neglecting the field dependence of the secondary emission coefficient γ, we have the Townsend ignition condition

$$\alpha d = \ln[(1+\gamma)/\gamma] = \Gamma \ . \tag{55}$$

With $E = U/d$ and the numerical result $E/p_0 = h(\alpha/E)$ of Fig. 5 (Table III), we obtain Paschen's law:

$$\frac{p_0 d}{\Gamma} = \frac{U/\Gamma}{h(\Gamma/U)} = k(U/\Gamma) \ , \tag{56}$$

shown in Fig. 6. As a consequence of the decrease of α for large E, this curve is bent back to the right on the LHS of the Paschen minimum and predicts an absolute minimum distance for ignition. This interesting result, which is in qualitative agreement with experimental evidence for He [24,26], should stimulate further investigations accounting for the full inhomogeneity of the EVDF in front of the electrodes.

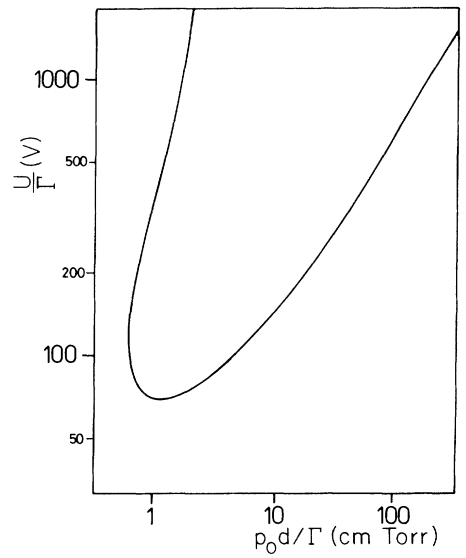

FIG. 6. Paschen curve $\alpha d = \ln[(1+\gamma)/\gamma] = \Gamma$ in He (U in V and $p_0 d$ in cm Torr).

ACKNOWLEDGMENTS

This investigation was performed under the auspices of the Sonderforschungsbereich 191 of the Deutsche Forschungsgemeinschaft. I would like to thank Professor G. Ecker for valuable discussions and suggestions.

APPENDIX A: ELECTRON CROSS SECTIONS IN He

For numerical illustrations we refer to a weakly ionized He plasma. To facilitate the comparison with corresponding results of Lagushenko and Maya [10], we start from the same simplified set of collision cross sections $q_{1\,\mathrm{el}}$ (elastic momentum transfer), q_{ex} (excitation of one electronic state), and q_i (ionization). The cross sections are given in units of Å^2, and $\varepsilon = mv^2/2$ is the electron energy in eV:

$$q_{1\,\mathrm{el}} = \frac{6.16}{1+(\varepsilon/15)^{3/2}} \ , \tag{A1}$$

$$q_{\mathrm{ex}} = \frac{2.82}{\varepsilon} \ln[1+[0.013+0.008(\varepsilon-\varepsilon_{\mathrm{ex}})]\varepsilon] \quad \text{with } \varepsilon_{\mathrm{ex}} = 20 \tag{A2}$$

$$q_i = \frac{19.8}{\varepsilon} \ln\left[1+\frac{0.046(\varepsilon-\varepsilon_i)\varepsilon}{70}\right] \quad \text{with } \varepsilon_i = 24 \ . \tag{A3}$$

The cross sections are plotted in Fig. 1. Evidently, q_{ex} and q_i become larger than $q_{1\,\mathrm{el}}$ at high electron energies. Adding q_{ex} and q_i to $q_{1\,\mathrm{el}}$, the runaway condition (19) is not fulfilled. With increasing electron energy, however, the energy loss in inelastic collisions becomes unimportant and we must account for the fact that scattering in inelastic collisions is *not* isotropic. In view of the simplified representation used here, we can refrain from the tedious task of finding reliable differential cross sections for e-He encounters and content ourselves with an estimate of the inelastic momentum-transfer cross section from the well-known Thompson model [27].

To this end, we add Eqs. (A2) and (A3) to the lumped inelastic cross section

$$q_{\mathrm{in}} = q_{\mathrm{ex}} + q_i \ , \tag{A4}$$

with the energy threshold $\varepsilon_{\mathrm{in}} = \varepsilon_{\mathrm{ex}}$. Within the Thompson model, the inelastic process is described by the interaction of the free electron with a shell electron at rest, and q_{in} can be approximated in the form

$$\tilde{q}_{\mathrm{in}} = 2\pi \int_{\Delta\varepsilon > \varepsilon_{\mathrm{in}}} \sigma_c(\varepsilon,\theta) \sin\theta \, d\theta \ , \tag{A5}$$

where

$$\sigma_c(\varepsilon,\theta) = \frac{\mathrm{const}}{\varepsilon^2} \sin^{-4}\frac{\theta}{2} \tag{A6}$$

is the Coulomb scattering cross section and

$$\Delta\varepsilon=\varepsilon\sin^2\frac{\theta}{2} \tag{A7}$$

is the energy transfer to the shell electron. In analogy to Eq. (A5), we can calculate the corresponding momentum-transfer cross section

$$\tilde{q}_{1\,\mathrm{in}}=2\pi\int_{\Delta\varepsilon>\varepsilon_{\mathrm{in}}}(1-\cos\theta)\sigma_c(\varepsilon,\theta)\sin\theta\,d\theta\ . \tag{A8}$$

Evaluating Eqs. (A5)–(A8), we obtain the ratio

$$\frac{\tilde{q}_{1\,\mathrm{in}}}{\tilde{q}_{\mathrm{in}}}=2\frac{\ln(\varepsilon/\varepsilon_{\mathrm{in}})}{\varepsilon/\varepsilon_{\mathrm{in}}-1}\ . \tag{A9}$$

The Thompson model is justified only for $\varepsilon\gg\varepsilon_{\mathrm{in}}$. Near the energy threshold ($\varepsilon\approx\varepsilon_{\mathrm{in}}$), we obtain, from Eq. (A9), $\tilde{q}_{1\,\mathrm{in}}\approx 2\tilde{q}_{\mathrm{in}}$ in contrast to the experimental evidence of isotropic scattering ($q_{1\,\mathrm{in}}\approx q_{\mathrm{in}}$). To account for this, we modify Eq. (A9) for $\varepsilon=O(\varepsilon_{\mathrm{in}})$ and use

$$q_{1\,\mathrm{in}}=2\frac{\ln(\varepsilon/\varepsilon_{\mathrm{in}})}{\varepsilon/\varepsilon_{\mathrm{in}}-\varepsilon_{\mathrm{in}}/\varepsilon}q_{\mathrm{in}} \tag{A10}$$

to calculate the inelastic momentum-transfer cross section from q_{in}. The entire momentum-transfer cross section q_1 used in the numerical evaluations and shown in Fig. 1 is given by

$$q_1=q_{1\,\mathrm{el}}+q_{1\,\mathrm{in}}\ . \tag{A11}$$

APPENDIX B: NUMERICAL SCHEME

The calculation of homogeneous EVDF's starts from Eqs. (25) and (31). Applying Eqs. (10), (13), (14), and (19), we obtain the system

$$f^1(v)=\frac{3}{Fv^2}\left\{\frac{S_R}{4\pi}+\frac{m}{M}n_0v^4q_{1\,\mathrm{el}}(v)f^0(v)+n_0\int_v^{v+\mathrm{in}}u^3q_{\mathrm{in}}(u)f^0(u)du\right\}, \tag{B1}$$

$$f^0(v)=\frac{n_0}{F}\int_v^{\infty}uq_1(u)f^1(u)du\ , \tag{B2}$$

where q_{in} is the cross section for one lumped inelastic process [see Eq. (A4)]. To reduce the number of grid points at high energy ($v\to v_R$) and to keep a sufficient resolution at low energy (energy-loss region), we use a numerical grid

$$v_n=nv_R/N \tag{B3}$$

equidistant in $v\propto\varepsilon^{1/2}$ and not, as usual, in ε. (This has the disadvantage that we have to interpolate evaluating the inelastic collision term.) Applying the trapezoidal law to Eq. (B1) and Simpson's law to Eq. (B2) results in a system of the form

$$f^1(v_n)=a_nf^0(v_n)+\sum_{\nu>n}a_{n,\nu}f^0(v_\nu)\ , \tag{B4}$$

$$f^0(v_n)=b_nf^1(v_n)+c_nf^1(v_{n+1})+d_nf^1(v_{n+2})+f^0(v_{n+2})\ . \tag{B5}$$

Taking starting values for $n\geq N-1$ from Eq. (33), $f^1(v_n)$ and $f^0(v_n)$ ($n=N-2,\ldots,1$) can be calculated successively from Eqs. (B4) and (B5). The grid point $n=0$ is omitted because of the singularity at $v=0$ discussed with Eq. (26).

To calculate the EVDF of a Townsend ionization avalanche, we replace Eqs. (B1) and (B2) by

$$g^1(v)=\frac{3}{Fv^2}\left\{\frac{S_R}{4\pi}+\hat{S}\right\}\quad\text{with}\ \hat{S}=\int_{v_R}^{v}u^2\hat{C}^0[g^0(u)]du\ , \tag{B6}$$

$$g^0(v)=\frac{n_0}{F}\int_v^{\infty}uq_1(u)g^1(u)du\ . \tag{B7}$$

According to Eqs. (10), (13), (14), and (49), $\hat{S}$ is explicitly given by

$$\hat{S}=n_0\left[\frac{m}{M}v^4q_{1\,\mathrm{el}}(v)g^0(v)+Q(v)+R(v)-e^{-(\alpha\varepsilon_{\mathrm{in}}/eE)}R(v_{+\mathrm{in}})\right]$$

$$\text{with}\ Q(v)=\frac{m\alpha}{MF}\int_v^{v_R}u^5q_{1\,\mathrm{el}}(u)g^0(u)du$$

$$\text{and}\ R(v)=\int_v^{v_R}u^3q_{\mathrm{in}}(u)g^0(u)du\ . \tag{B8}$$

(Formally, Q shows a weak singularity for $v\to\infty$. Actually, however, this term can always be neglected in comparison to the first elastic term or to R.) The numerical evaluation follows the scheme of the homogeneous case. Again, we omit the grid point $n=0$ because of a singularity for $v\to 0$. [In contrast to the homogeneous case, this (unimportant) singularity has no justification by the model assumptions and could, in principle, be avoided by a different choice of the integration constants in Eqs. (B6) and (B7). Such a choice, however, would result in an isotropic distribution $g^0\to$const for $v\to\infty$. Actually, the problem of appropriate integration constants cannot be solved consistently within the two-term SHE.]

Simultaneously with the EVDF, we have to determine α by iteration. Increasing the reduced field step by step, suitable start values are obtained by $\alpha=0$ for low E/n_0 and from the preceding step for higher values of E/n_0.

APPENDIX C: SMALL-ANGLE SCATTERING

Neglecting energy exchange, Boltzmann's collision term for angular scattering in electron-atom encounters becomes

$$C[f]=n_0\int\{f(v,\mu')-f(v,\mu)\}v\sigma(v,\theta)\sin\theta\,d\theta\,d\phi$$
$$=n_0 v\sum_{k=1}^{\infty}\frac{1}{k!}\frac{\partial^k f(v,\mu)}{\partial\mu^k}$$
$$\times\int(\mu'-\mu)^k\sigma(v,\theta)\sin\theta\,d\theta\,d\phi\ , \qquad \text{(C1)}$$

where θ is the deflection angle and ϕ the azimuthal angle in the relative system of a binary collision. Inserting the precollision direction cosine

$$\mu'=\mu\cos\theta+(1-\mu^2)^{1/2}\sin\theta\cos\phi \qquad \text{(C2)}$$

and neglecting contributions $\propto\theta^4$ and higher order in θ, we obtain Eq. (34) by straightforward integration.

[1] V. L. Ginzburg, and A. V. Gurevich, Usp. Fiz. Nauk **70**, 201 (1960) [Sov. Phys.—Usp. **3**, 115 (1960)].

[2] I. P. Shkarovsky, T. W. Johnston, and M. P. Bachynski, *The Particle Kinetics of Plasmas* (Addison-Wesley, Reading, MA, 1966), Chap. 3.

[3] B. I. Davydov, Phys. Z. Sowjetunion **8**, 59 (1935).

[4] R. M. Thomson, K. Smith, and A. R. Davies, Comput. Phys. Commun. **11**, 369 (1976).

[5] A. V. Phelps and L. C. Pitchford, Phys. Rev. A **31**, 2932 (1985).

[6] R. Winkler, G. L. Braglia, A. Hess, and J. Wilhelm, Beitr. Plasmaphys. **25**, 351 (1985).

[7] H. Dreicer, Phys. Rev. **115**, 283 (1959).

[8] G. Ecker and K. G. Müller, Z. Naturforsch. Teil A **16**, 246 (1961).

[9] K. G. Müller, Z. Phys. **169**, 432 (1962).

[10] R. Lagushenko and J. Maya, J. Appl. Phys. **55**, 3293 (1984).

[11] H. B. Valentini, Contrib. Plasma Phys. **27**, 331 (1987).

[12] *Handbook of Mathematical Functions,* edited by M. Abramowitz and I. A. Stegun, (Dover, New York, 1965), Chaps. 8 and 22.

[13] M. N. Rosenbluth, W. M. MacDonald, and D. L. Judd, Phys. Rev. **107**, 1 (1957).

[14] Yu. M. Kagan and R. I. Lyagushchenko Zh. Tekh. Fiz. **34**, 821 (1964) [Sov. Phys.—Tech. Phys. **9**, 627 (1964)].

[15] S. Yoshida, A. V. Phelps, and L. C. Pitchford, Phys. Rev. A **27**, 2858 (1983).

[16] I. B. Levinson, Fiz. Tverd. Tela (Leningrad) **6**, 2113 (1964) [Sov. Phys.—Solid State **6**, 1665 (1965)].

[17] L. Stenflo, Plasma Phys. **8**, 665 (1966).

[18] G. Cavalleri and S. L. Paveri-Fontana, Phys. Rev. A **6**, 327 (1972).

[19] A. V. Gurevich, Zh. Eksp. Teor. Fiz. **39**, 1296 (1960) [Sov. Phys.—JETP **12**, 904 (1961)].

[20] A. N. Lebedev, Zh. Eksp. Teor. Fiz. **48**, 1993 (1965) [Sov. Phys.—JETP **21**, 931 (1965)].

[21] E. H. Holt and R. E. Haskell, *Foundations of Plasma Dynamics* (Macmillan, New York, 1965), Chap. 9.2.

[22] See *Handbook of Mathematical Functions,* Ref. [12], Chaps. 13 and 22.

[23] E. Gerjuoy and G. W. Stuart, Phys. Fluids **3**, 1008 (1960).

[24] A. V. Phelps, in *Proceedings of the XVIII International Conference on Phenomena in Ionized Gases,* edited by W. T. Williams (Swansea, Philadelphia, 1987), p. 2.

[25] A. V. Phelps, B. M. Jelenković, and L. C. Pitchford, Phys. Rev. A **36**, 5327 (1987).

[26] A. V. Phelps and B. M. Jelenković, Phys. Rev. A **38**, 2975 (1988).

[27] J. J. Thompson, Philos. Mag. **23**, 449 (1912).